Utilization of Ghost Reflections by Echo-deblending

Berkhout, Guus; Blacquière, Gerrit

DOI
10.3997/2214-4609.201601216

Publication date
2016

Document Version
Final published version

Published in
78th EAGE Conference and Exhibition 2016, Vienna, Austria

We SRS3 13

Utilization of Ghost Reflections by Echo-deblending

A.J. Berkhout (Delft University of Technology) & G. Blacquiere* (Delft University of Technology)

SUMMARY

It is shown that deghosting is actually a data-adaptive deblending process. This special deblending process is nonlinear and can be carried out such that the effect of noise is minimized. Our algorithm is explained and illustrated with examples.

Introduction

The source and detector ghost effects in marine acquisition cause angle-dependent notches in the spectrum and severe attenuation of the low frequencies leading to large sidelobes of the wavelet. Ghost suppression removes these effects at the detector side, see e.g., Soubaras (2010), Ferber et al. (2013), and Beasley et al. (2015), and at the source side, see e.g., Mayhan and Weglein (2013) and Amundsen and Zhou (2013). Due to the deep notches in the wavenumber frequency domain, deghosting involves a large amplification in the notch areas, which may be detrimental to the signal-to-noise ratio (SNR) of the final result. In our research we pay special attention to deghosting at the source side. In a first step we separate the deghosting process in two independent processes: zero-phasing and ceiling-driven amplitude shaping. The phase is always treated correctly, whereas the amplitude corrections are maximized by a ceiling, depending on the SNR. After this first step, the residue is treated with a second, nonlinear signal-recovering step in the notch areas. The output of the algorithm consists of the response of the real sources as well as the response of the ghost sources. Our deghosting algorithm represents an echo-deblending process.

Deghosting: forward model

In marine acquisition, the sources are towed at some depth $z_s = z_s(x,y)$. Due to the strong reflectivity at the water surface (level z_0) two source wavefields are generated: one is directly travelling down, the second is going up, reflects at the water surface and then travels down, causing the ghost response, see Figure 1. The transmitted source wavefield is the sum of the two. Using the matrix notation (Berkhout, 1985), the process can be formulated as follows for each frequency component:

$$\mathbf{S}^+(z_s) = \mathbf{S}_0^+(z_s) + \mathbf{W}^+(z_s,z_0)\mathbf{R}^{\cap}(z_0,z_0)\mathbf{W}^-(z_0,z_s)\mathbf{S}_0^-(z_s). \tag{1}$$

Matrices $\mathbf{W}^-$ and $\mathbf{W}^+$ describe up- and downward extrapolation, matrix $\mathbf{R}^{\cap}$ describes the angle- and frequency-dependent surface reflectivity and matrices $\mathbf{S}^-$ and $\mathbf{S}^+$ describe the source directivity and strength in the up- and downward direction. The subscript 0 refers to the ghost-free situation. If the source properties in the down- and upward direction are the same, equation 1 can be written as:

$$\mathbf{S}^+(z_s) = \mathbf{G}^+(z_s,z_s)\mathbf{S}_0^+(z_s), \tag{2}$$

where matrix $\mathbf{G}^+$ is the source-side ghost operator given by:

$$\mathbf{G}^+(z_s,z_s) = [\mathbf{I}(z_s) + \mathbf{W}^+(z_s,z_0)\mathbf{R}^{\cap}(z_0,z_0)\mathbf{W}^-(z_0,z_s)]. \tag{3}$$

Before going to deghosting, let us first have a look at ghost operator $\mathbf{G}^+$ and its properties. In Figure 2 the operator is shown for various surface reflectivies and source depths in the fk-domain. The larger the source depth the more notches and the larger the surface reflectivity the deeper the notches. In practical cases - although the notches may be deep - the amplitude of the ghost operator is never zero.
Finally, the model for seismic data including the source ghost is:

$$\mathbf{P}^-(z_0;z_s) = \mathbf{X}^{\cup}(z_0,z_s)\mathbf{G}^+(z_s,z_s)\mathbf{S}_0^+(z_s), \tag{4}$$

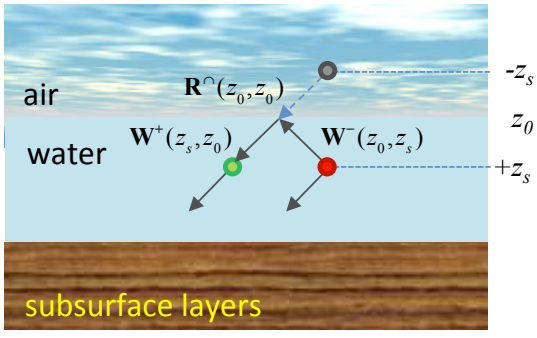

Figure 1 *Two source wavefields are generated: the first is travelling down directly, the second is going up, getting reflected at the surface and then travelling down. The total generated wavefield is the sum.*

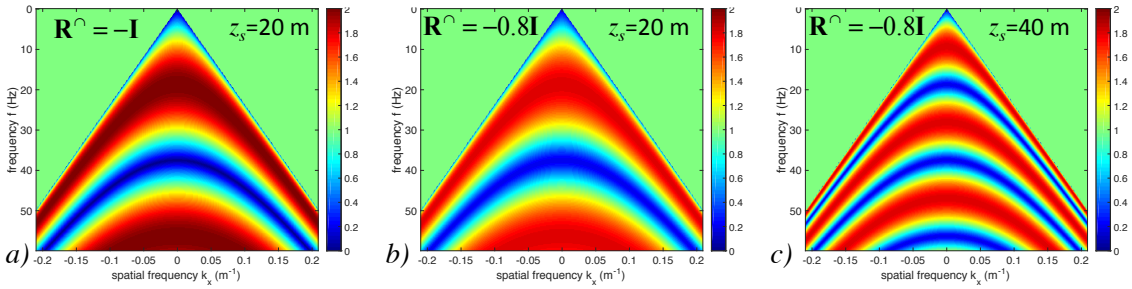

Figure 2 *Amplitude of the ghost operator* $\mathbf{G}^{+}(z_s, z_s)$ *for various* z_s *and* $\mathbf{R}^{\cap}$ *in the fk-domain.*

where the detectors are located at z_0. Here $\mathbf{X}^{\cup}$ is the Earth transfer function. Each column of $\mathbf{P}^{-}$ is a monochromatic shot record and each row a monochromatic receiver gather.
The model can be easily extended to contain the ghost response related to detectors at level $z_d(x,y)$ as well:

$$\mathbf{P}(z_d; z_s) = \mathbf{D}_0^{-}(z_d)\mathbf{G}^{-}(z_d, z_d)\mathbf{X}^{\cup}(z_d, z_s)\mathbf{G}^{+}(z_s, z_s)\mathbf{S}_0^{+}(z_s), \tag{5}$$

where $\mathbf{D}_0^{-}$ is the detector matrix. Note that in practice, $\mathbf{S}_0^{+}$ and $\mathbf{D}_0^{-}$ may be very different. In the remainder of this paper we focus on the source-side ghost.

Source deghosting: inverse model

The action of source deghosting means that the data-with-ghost $\mathbf{P}^{-}(z_0; z_s)$ is turned into ghost-free data $\mathbf{P}_0^{-}(z_0; z_s) = \mathbf{X}^{\cup}(z_0, z_s)\mathbf{S}_0^{+}(z_s)$. Comparing this expression with equation 4 makes clear that deghosting corresponds to:

$$\mathbf{P}_0^{-}(z_0; z_s) = \mathbf{P}^{-}(z_0; z_s)[\mathbf{S}_0^{+}(z_s)]^{-1}[\mathbf{G}^{+}(z_s)]^{-1}\mathbf{A}(z_s), \tag{6}$$

where $\mathbf{A}$ refers to the optimum seismic bandwidth. In the first step, we carry out the inversion of ghost operator matrix $\mathbf{G}^{+}$ via a two-stage procedure:

$$[\mathbf{G}^{+}(z_s, z_s)]^{-1} = min\left[ceiling; \frac{1}{||\mathbf{G}^{+}(z_s, z_s)||^2}\right][\mathbf{G}^{+}(z_s, z_s)]^{H}, \tag{7}$$

where superscript H denotes the conjugate transpose and where *ceiling* is the maximum amplitude correction allowed. The first stage aims at 'zero-phasing' and corresponds to applying the numerator of equation 7, whereas the second stage, 'ceiling-driven amplitude shaping', corresponds to applying the denominator. The zero-phasing step guarantees that the phase of the result is always perfect both inside and outside the notch areas, see Figure 3c. The ceiling-driven amplitude shaping gives an optimum result for a given SNR: there is no error outside notch areas, but inside the notch area the amplitude correction is limited. The key is to balance these limited amplitude corrections and the noise content in such a way that neither of them is dominant, see the example in Figure 3d and 3e where two ceilings have been applied of 1 and 40 respectively. Applying a ceiling of 1 clearly leads to a less noisy result, but the limited amplitude correction becomes visible. If the ceiling is increased to 40 (Figure 3e) these amplitude limitations are reduced at the cost of some increase of the noise. The residue (the non-perfect result in the notch areas) is input to the next roundtrip of the closed-loop scheme in Figure 5 (Berkhout and Blacquière, 2015). The result is shown in Figure 3e. The benefits of the method become even more clear if more noise is present as is illustrated in Figure 4. Finally, we remark that for a proper application of equation 7 both the water velocity and the surface reflectivity need be known accurately. They are estimated during the deghosting process (Berkhout and Blacquière, 2015).

Spatial sampling and deghosting

Going back to equation 6, apart from the inversion of ghost matrix $\mathbf{G}^{+}$, also the inverse of source matrix $\mathbf{S}_0$ has to be computed. This clearly illustrates the importance of a wide-band source and a proper spatial sampling. Examples of carpet shooting (Walker et al., 2014) at the source side, and interpolation of

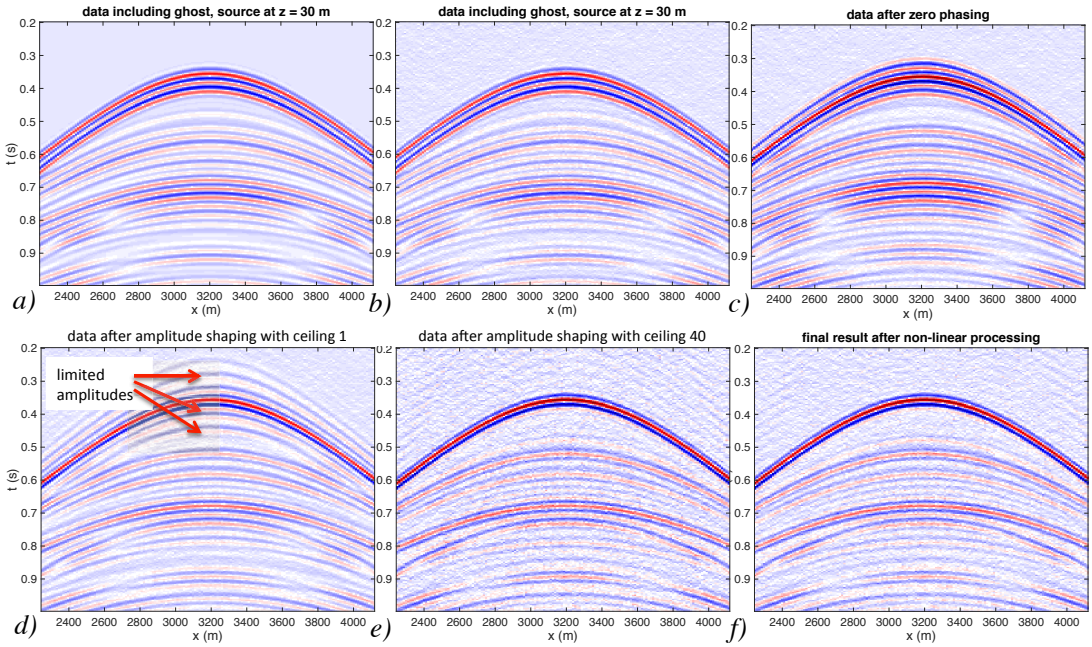

Figure 3 *a. Input with no noise, b. input with a small amount of noise, SNR 30 dB, c. output with source at $+z_s$: zero-phasing only, d. output with ceiling of 1, e. output with ceiling of 40, f. output after nonlinear processing. We do not show the output at $-z_s$ because it looks very similar.*

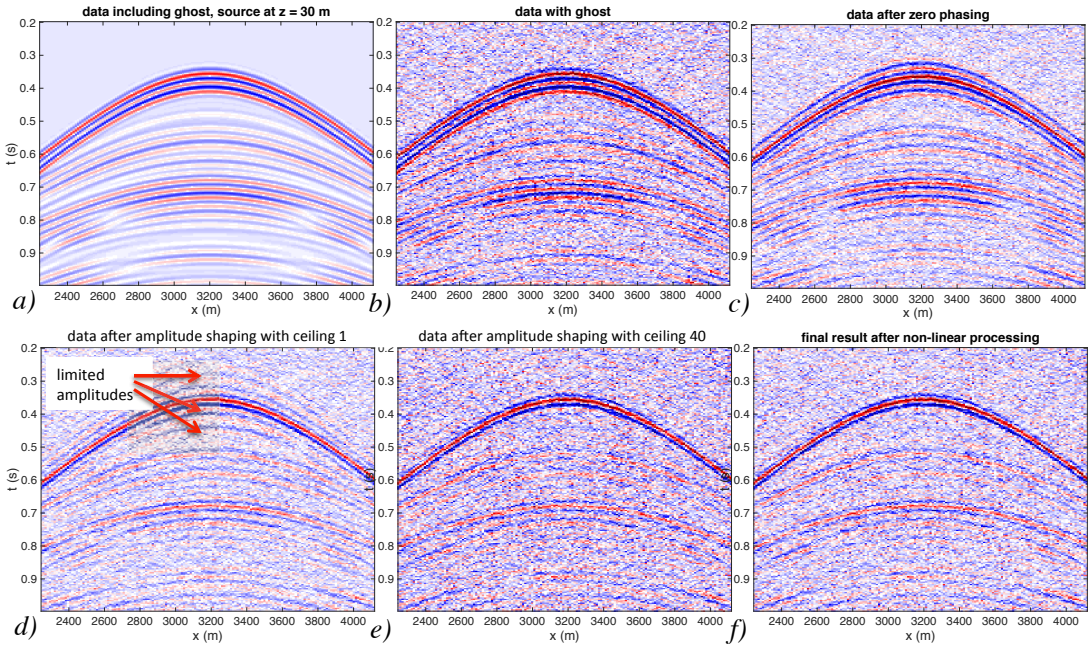

Figure 4 *See figure 3, but now more noise has been added: SNR = 15 dB.*

multi-sensor data (Letki and Spjuth, 2014) at the detector side, allow practical deghosting in the space-frequency domain.

In addition, we propose that the low frequencies are treated with special care in (re)processing. Low frequencies suffer from the notch at 0 Hz. From the current focus on broadband acquisition and broadband (re)processing, it is well-known that the low frequencies are very important: they reduce the sidelobes of the wavelet and enhance the seismic resolution. The coarse sampling in conventional acquisition, in particular at the source side, is mostly affecting the high frequencies. During the presentation it will be shown how to give the low-frequencies a special treatment.

Concluding remarks

Our deghosting algorithm represents a deblending process: each shot record is decomposed into a response from the real source at $+z_s$ and a response from the ghost source at $-z_s$.

The uniqueness of our algorithm is that the phase is correctly treated for all frequencies (no compromise inside and outside the notch areas) and that for amplitude stabilization there is no compromise outside the notch areas. An extra nonlinear step aims at recovering the signal component *inside* the notch areas.

Acknowledgements

We acknowledge the sponsors of the Delphi consortium for the stimulating discussions and support.

References

Amundsen, L. and Zhou, H. [2013] Low-frequency seismic deghosting. *Geophysics*, **78**, WA15–WA20.
Beasley, C.J., Coates, R.T., Flath, P. and Castellanos, C. [2015] Slanted cable marine acquisition and wave-equation receiver deghosting. *SEG Technical Program Expanded Abstracts*, 105–109.
Berkhout, A. and Blacquière, G. [2015] Deghosting by echo-deblending. *Geophysical Prospecting*.
Berkhout, A.J. [1985] *Seismic migration, Volume A: Theoretical Aspects, 3rd edn.* Elsevier.
Ferber, R., Caprioli, P. and West, L. [2013] L1 pseudo-V_z estimation and deghosting of single-component marine towed-streamer data. *Geophysics*, **78**(2), WA21–WA26.
Letki, L.P. and Spjuth, C. [2014] Quantification of Wavefield Reconstruction Quality from Multisensor Streamer Data Using a Witness Streamer Experiment. EAGE.
Mayhan, J.D. and Weglein, A.B. [2013] First application of Green's theorem-derived source and receiver deghosting on deep-water Gulf of Mexico synthetic (SEAM) and field data. *Geophysics*, **78**(2), WA77–WA89.
Soubaras, R. [2010] Deghosting by joint deconvolution of a migration and a mirror migration. *SEG Technical Program Expanded Abstracts*, **29**(1), 3406–3410.
Walker, C., Monk, D. and Hays, D. [2014] Blended Source - the Future of Ocean Bottom Seismic Acquisition. EAGE.

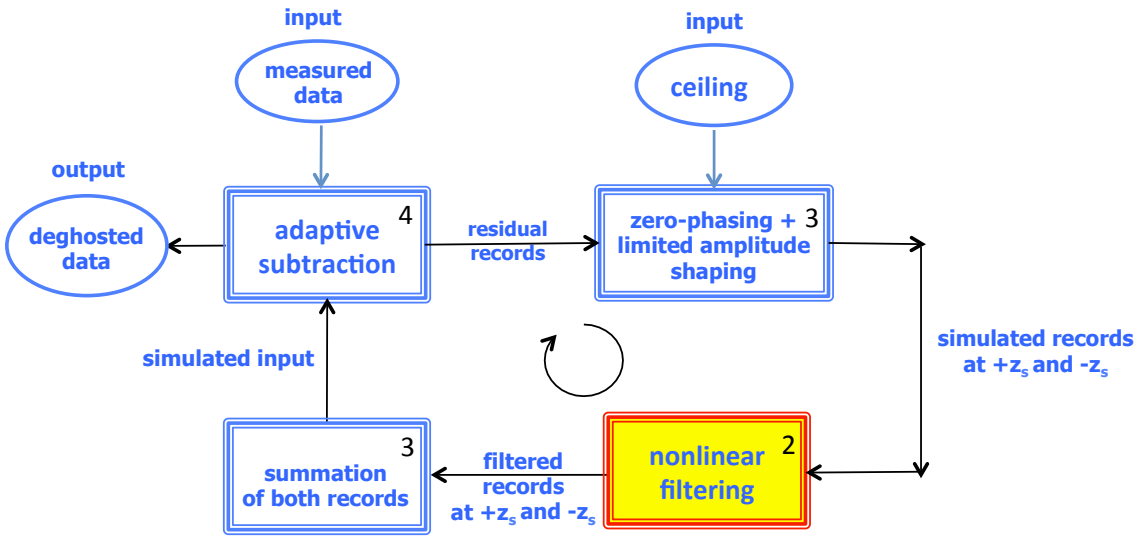

Figure 5 *Our nonlinear echo-deblending method is formulated as a closed-loop process, meaning that the ouput and input are connected via a feedback loop.*